

# Electronic structure and Jahn-Teller effect in GaN:Mn and ZnS:Cr

F. Viro, <sup>1</sup> R. Hayn, <sup>1</sup> and A. Boukourt <sup>1,2</sup>

<sup>1</sup>*Institut Matériaux Microélectronique Nanosciences de Provence, Faculté St. Jérôme, Case 142, F-13397 Marseille Cedex 20, France*

<sup>2</sup>*Mostaganem University, Faculty of Science and Technology, Genie Electric Department 27000, Algeria*

(Dated: October 31, 2018)

## Abstract

We present an ab-initio and analytical study of the Jahn-Teller effect in two diluted magnetic semiconductors (DMS) with  $d^4$  impurities, namely Mn-doped GaN and Cr-doped ZnS. We show that only the combined treatment of Jahn-Teller distortion and strong electron correlation in the  $3d$  shell may lead to the correct insulating electronic structure. Using the LSDA+ $U$  approach we obtain the Jahn-Teller energy gain in reasonable agreement with the available experimental data. The ab-initio results are completed by a more phenomenological ligand field theory.

PACS numbers: 75.50.Pp, 71.23.An, 71.55.-i, 71.70.Ej

## I. INTRODUCTION

The Jahn-Teller effect of impurity ions in semiconductors with degenerate ground state is well known since long time. Most of its theoretical treatments were based on crystal field theory. Actually, the class of diluted magnetic semiconductors regains a lot of interest in connection with the search for new materials for spintronics applications. For example, high Curie temperatures were predicted in GaN:Mn.<sup>1</sup> Corresponding experimental<sup>2</sup> or ab-initio studies<sup>3</sup> seemed to confirm these predictions. However, the experimental results are very disputed since they might be caused by small inclusions of secondary phases.<sup>4</sup> And also most of the previous ab-initio studies obtained a partially filled band of only one spin direction at the Fermi level (half-metallic behavior) which will be shown to be an artifact of those calculations. Actually, the Mn ion changes its valence in the chemical series from GaAs:Mn, via GaP:Mn to GaN:Mn.<sup>5</sup> It is Mn<sup>2+</sup> in GaAs:Mn (for a sufficiently high Mn-concentration)<sup>6</sup> which leads to hole doping, but it remains Mn<sup>3+</sup> in GaN:Mn. And the Jahn-Teller effect is crucial to stabilize Mn<sup>3+</sup>. As will be shown below, only the combined treatment of Jahn-Teller effect and strong electron correlations leads to the correct electronic structure. The electron correlations turn out to be the leading interaction, but the Jahn-Teller effect is necessary to break the symmetry.

We present here a combined ab-initio and crystal field theory of magnetic ions in II-VI or III-V semiconductors. As representative examples we treat the  $3d^4$  ions Mn<sup>3+</sup> in GaN and Cr<sup>2+</sup> in ZnS. The first one is chosen because of its actual interest for spintronic applications and the second one since it is a very well studied model system for the Jahn-Teller effect of  $d^4$  ions.<sup>7</sup> Our ab-initio results are in good agreement with the experimental data, but only if we include properly the effects of the electron correlations in the  $3d$  shell. For that purpose we use the LSDA+ $U$  method. The resulting electronic structure corrects previous electronic structure calculations (which did not take into account the combined effect of Jahn-Teller distortion and Coulomb correlation, neither for Mn-doped GaN<sup>8,9</sup> nor for Cr-doped ZnS<sup>10,11</sup>) in a dramatic way: instead of half-metallic behavior we obtain an insulating ground state with a considerable excitation gap. Similar results for GaN:Mn were reported earlier but using different methods than in our study.<sup>5,12</sup> In a second step, to make contact with the traditional literature on that subject, we connect our ab-initio results with crystal field theory. We obtain the complete set of crystal field parameters in good agreement with

previous optical measurements.<sup>7,13,14</sup>

We treat the host crystals in zinc-blende phase. Both magnetic ions are in the  $3d^4$  configuration. The electronic level is split by a cubic crystal field created by the first nearest neighbors (ligands) of the transition metal ion. But it remains partially filled and the Jahn-Teller effect may occur which induces the splitting of the partially filled level due to displacements of the ligands around the transition metal ion. The local symmetry of the crystal is reduced and the total energy of the supercell is minimized. The energy gain is denoted as  $E_{JT}$ .

## II. METHOD OF CALCULATION

Our calculations are performed using the full potential local orbital (FPLO)<sup>15</sup> method with the LSDA+ $U$  (local spin density approximation with strong Coulomb interaction)<sup>16</sup> approximation in the atomic limit scheme. The lattice constants are optimized for the pure semiconductors using the LSDA method,  $a_0 = 4.48 \text{ \AA}$  for GaN and  $a_0 = 5.32 \text{ \AA}$  for ZnS. To study the Jahn-Teller effect, we use a supercell of 64 atoms in zinc blende phase, and a  $4 \times 4 \times 4$  k-point mesh. The LSDA+ $U$  parameters are introduced as Slater parameters : for Mn (see Ref. 16),  $F^2 = 7.41 \text{ eV}$ ,  $F^4 = 4.63 \text{ eV}$  and for Cr (see Ref. 17),  $F^2 = 7.49 \text{ eV}$ ,  $F^4 = 4.68 \text{ eV}$ . The  $F^0$  parameter is equal to  $U$ , and is chosen to be 4 eV. This value is in good agreement with other works and it corresponds to the value which gives the maximum splitting of the triplet state in  $D_{2d}$  symmetry. We have verified that our results are not very sensitive to the actual choice of the  $U$  parameter. The value  $U = 4 \text{ eV}$  gives representative results for a rather large range of  $U$  parameters reaching from 3 up to 8 eV.

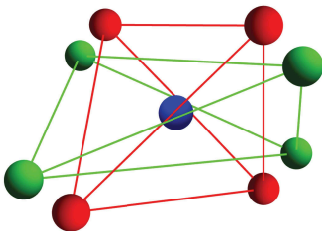


FIG. 1: (Color online) Schematic drawing of a tetragonal distortion from  $T_d$  (red spheres) to  $D_{2d}$  (green spheres).

The transition metal ions (Mn or Cr) substitute one atom in the center of the crystal and

there is a complete tetrahedron of ligands around the magnetic ion. Without distortion, the tetrahedron is in the  $T_d$  symmetry group (cubic). By symmetry, there are two tetragonal (point groups  $C_{2v}$  and  $D_{2d}$ ) and one trigonal ( $C_{3v}$ ) possible Jahn-Teller distortions. We have verified that the most important energy gain is obtained with the pure tetragonal distortion where the symmetry reduces from  $T_d$  to  $D_{2d}$ . That is in agreement with a previous study of the Jahn-Teller effect in GaN:Mn where, however, the electron correlation had not been taken into account.<sup>18</sup> The schematic displacement of ligands is represented in Fig. 1, it is defined by  $\delta_x = \delta_y \neq \delta_z$ .

### III. AB-INITIO RESULTS

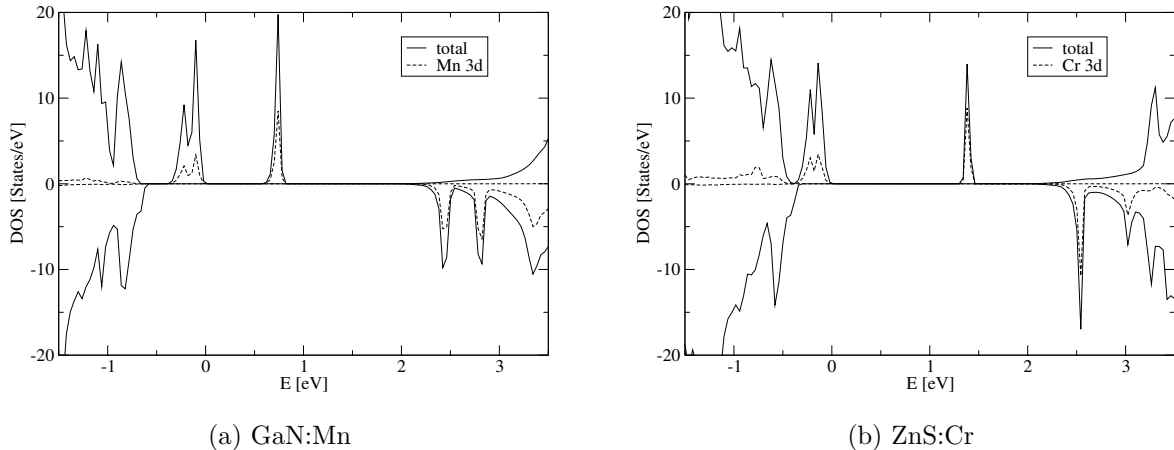


FIG. 2: Partial density of states (DOS) of the two DMS. The results were obtained with the LSDA+ $U$  method ( $U = 4$  eV). The dashed line represents the partial 3d DOS of the transition metal ion and the solid line represents the total DOS. The Fermi level is set to 0 eV.

To study the Jahn-Teller distortion we use a supercell of 64 atoms. We performed a series of calculations with different displacements of the ligands around the impurity in order to find the configuration which minimizes the total energy of the supercell. The preferred configuration is of  $D_{2d}$  symmetry and the results for the density of states (DOS) are presented in Fig. 2. For Mn-doped GaN, the distance between Mn and N is 1.942 Å (with cubic symmetry, it is 1.937 Å) with  $\delta_x = 1.68$  pm and  $\delta_z = 1.76$  pm. The Jahn-Teller effect induces a lowering of the total energy by 38.13 meV and a splitting of the triplet state

by 0.81 eV. For Cr-doped ZnS, the results are similar, the distance Cr-S is 2.314 Å (2.304 Å without Jahn-Teller effect), with  $\delta_x = 3.36$  pm and  $\delta_z = -0.32$  pm. The total energy decreases by 58.1 meV and the splitting of the triplet level is 1.44 eV.

Without  $U$ , in the LSDA method, we also find a Jahn-Teller effect for GaN:Mn but the energy gain is smaller by nearly two orders of magnitude, only 0.71 meV. In the LSDA method all the  $3d$  levels are located in the gap with a rather small mixing to the  $2p$  orbitals. Without Jahn-Teller effect, there is a small band of  $t_{2g}$  character which is partially filled and one finds half-metallic behavior. The Hubbard correlation opens up a considerable gap. The empty state (singlet) is mainly of  $3d$  character for the two compounds and the doublet, just below the Fermi level is mainly of  $2p$  character originating from ligand orbitals. That change of orbital character arises since the LSDA+ $U$  method pushes the occupied  $3d$  levels much lower in energy than in the LSDA method. As a consequence, the transition to the first excited state has a considerable  $p$ - $d$  character and should be visible as an optical interband transition. That allows a reinterpretation of the optical transition at 1.4 eV (for GaN:Mn) which is usually considered as a pure  $d$ - $d$  transition.<sup>13</sup> In agreement with a proposal of Dietl it corresponds to a transition from the  $d^4$  configuration to  $d^5$  and ligand hole.<sup>19</sup>

There are two peaks in the unoccupied, minority DOS at about 2.5 eV for GaN:Mn. They correspond to crystal field split  $3d$  levels which were well seen in X-ray absorption spectroscopy. Up to now, they were interpreted by means of a LSDA calculation,<sup>20</sup> but our DOS shows that these peaks occur also in the more realistic LSDA+ $U$  approach where, however, a detailed calculation of the matrix element effects (which was performed in Ref. 20) is still lacking.

For GaN:Mn, the total magnetic moment is equal to  $4\mu_B$ , corresponding to  $S = 2$ . That fits well with the ionicity 3+ for manganese. The local magnetic moment at the manganese site is slightly enhanced  $M_{Mn} = 4.042\mu_B$  which is compensated by small induced magnetic moments of opposite sign at the neighboring ligands and further neighbors.

Another interesting result is presented in Fig. 3. In this case we introduced the local Coulomb correlation but no lattice deformation. The local cubic symmetry was however broken by the occupation of the triplet state. The calculation still shows an insulating case with nearly the same splitting of the triplet state. This observation is not visible within the LSDA method. Therefore, we can say that the splitting of the triplet state is mainly due to the strong correlation of  $3d$  electrons. The Jahn-Teller distortion introduces a small

additional splitting of the triplet state : 60 meV for Mn-doped GaN and  $-11.4$  meV for Cr-doped ZnS. This interpretation is confirmed by a pure LSDA calculation, because it gives an identical value of the splitting with the same ligand coordinates. A negative value of the splitting corresponds to a stretching of the tetrahedron along the z axis (Fig. 3(b)).

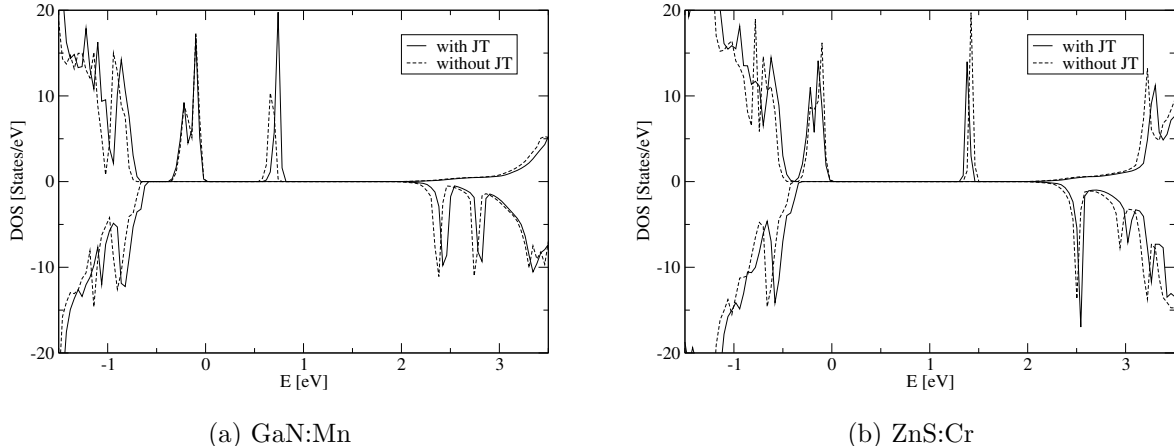


FIG. 3: DOS resulting from the LSDA+ $U$  calculation ( $U = 4$  eV). The dashed line represents the DOS without Jahn-Teller distortion, and the solid line represents the DOS with Jahn-Teller effect but by breaking the local cubic symmetry. The Fermi level is set to 0 eV.

#### IV. LIGAND FIELD THEORY

For a deeper understanding of the Jahn-Teller effect we treat it also in ligand field theory. In that theory, the degeneracy of the impurity  $3d$  level is split due to hybridization with the neighboring ligands. In the following we neglect the electrostatic contributions which will be shown to be justified for GaN:Mn and to a lesser extent for ZnS:Cr. When the  $3d$  ion is in the center of an ideal tetrahedron, the cubic crystal field splits this level into a triplet state and a doublet state. The distance separating these two levels is denoted as  $\Delta_q$ . Then, the Jahn-Teller effect splits the doublet state into two singlet states, and the triplet state into a doublet state and a singlet state. The distance between these levels is denoted as  $\Delta_{5T_2}$  (shown in Fig. 4). The local Hamiltonian in ligand field or crystal field theory can be

expressed as

$$\begin{aligned}
 H_{CF} &= H_{cub} + H_{tetra} \\
 &= B_4(O_4^0 + 5O_4^4) + (B_2^0 O_2^0 + B_4^0 O_4^0)
 \end{aligned}
 \tag{1}$$

where  $B_k^q$  and  $O_k^q$  are Steven's parameters and Steven's operators, respectively.<sup>21</sup> The first part represents the Hamiltonian of an ideal tetrahedron and the second describes the linear Jahn-Teller effect. The eigenvalues of  $H_{CF}$  correspond to the  $3d$  electronic levels of the magnetic ion (they represent the spectrum).  $B_4$  is the parameter of the cubic crystal field, and it is equal to  $\Delta_q/120$ .

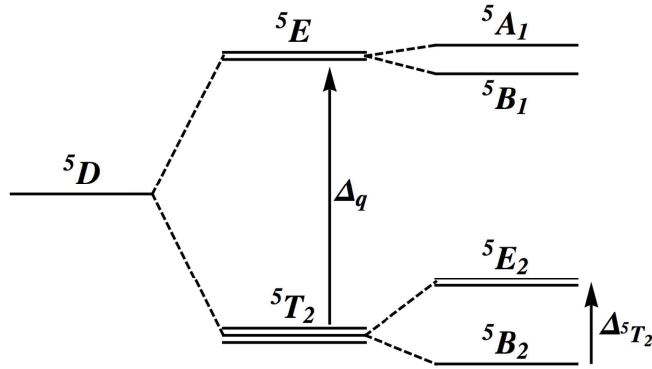


FIG. 4: Schematic multiplet spectrum for a transition metal ion in  $d^4$  configuration. From left to right,  ${}^5D$ : isolated ion, cubic crystal field splitting, and level splitting due to the Jahn-Teller distortion.

The crystal field Hamiltonian (1) has the same form for the one-particle problem (with parameters  $B_4$ ,  $B_2^0$ , and  $B_4^0$ ) or for the  $3d^4$  multiplet (with parameters  $\tilde{B}_4$ ,  $\tilde{B}_2^0$ , and  $\tilde{B}_4^0$ ).<sup>21,22</sup> The fundamental multiplet state is  ${}^5D$  ( $L = 2$  and  $S = 2$ ). In this fundamental state, the orbital moment for one electron ( $l = 2$ ) is equal to the total orbital moment. This particular case induces that the one electron spectrum is opposite to the multiplet spectrum (ex :  $\tilde{B}_4 = -B_4$ ). In the superposition model<sup>22-24</sup> the crystal field Hamiltonian (1) can be calculated by adding up the hybridization contributions of all the ligands. Then, the matrix elements of  $H_{CF}$  with respect to the projection  $m_L$  of the total orbital momentum  $L = 2$

are given by

$$\begin{aligned}
V_{m_L, m'_L} = & \sum_i \left[ A_{m'_L, m_L} b_4(R_i) Y_4^{m_L - m'_L}(\theta_i, \phi_i) \right] \\
& + \sum_i \left[ B_{m'_L, m_L} b_2(R_i) Y_2^{m_L - m'_L}(\theta_i, \phi_i) \right] \\
& + \sum_i \left[ b_0(R_i) \delta_{m'_L, m_L} \right]
\end{aligned} \tag{2}$$

with

$$\begin{aligned}
A_{m'_L, m_L} &= \frac{(-1)^{m'_L} 5\sqrt{4\pi}}{27} C_{-m'_L, m_L}^{224} C_0^{224} \\
B_{m'_L, m_L} &= \frac{(-1)^{m'_L} \sqrt{4\pi}}{\sqrt{5}} C_{-m'_L, m_L}^{222} C_0^{222}
\end{aligned} \tag{3}$$

and where  $C_{m_1 m_2}^{j_1 j_2 J}$  are Clebsch-Gordon coefficients and  $Y_L^{m_L, m'_L}$  are spherical harmonics. The  $i$  index corresponds to the ligand number. The axis system is defined in Fig. 5.

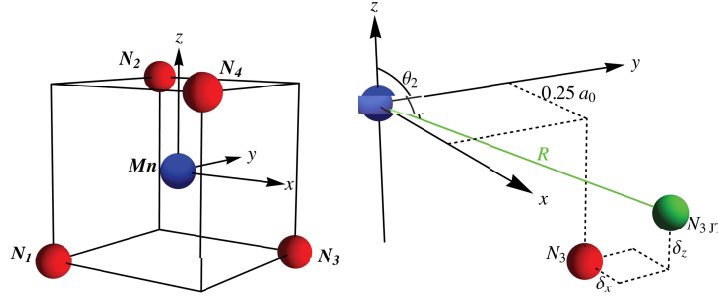


FIG. 5: (Color online) Definition of coordinate axes and lattice displacements used in the present work. Example of  $\text{MnN}_4$ .

In identifying the eigenvalues of  $H_{CF}$  with the equivalent values of  $V_{m_L, m'_L}$ , we obtain the expressions of the Steven's parameters as a function of the ligand coordinates

$$\begin{aligned}
\tilde{B}_4 &= \frac{-b_4(R) \tilde{Y}_4^4(\theta_2, \theta_3)}{120} \\
\tilde{B}_4^0 &= \frac{b_4(R)}{84} \left( \frac{\tilde{Y}_4^0(\theta_2, \theta_3)}{12} + \frac{7\tilde{Y}_4^4(\theta_2, \theta_3)}{12} \right) \\
\tilde{B}_2^0 &= \frac{-2b_2(R) \tilde{Y}_2^0(\theta_2, \theta_3)}{49}
\end{aligned} \tag{4}$$

with

$$\begin{aligned}
\tilde{Y}_4^0(\theta_2, \theta_3) &= 6 - 30(\cos^2 \theta_2 + \cos^2 \theta_3) + 35(\cos^4 \theta_2 + \cos^4 \theta_3) \\
\tilde{Y}_4^4(\theta_2, \theta_3) &= \sin^4 \theta_2 + \sin^4 \theta_3 \\
\tilde{Y}_2^0(\theta_2, \theta_3) &= -2 + 3 \cos^2 \theta_2 + 3 \cos^2 \theta_3 \\
b_2(R) &= \frac{\hbar^4 R_d^3}{\Delta_{pd} m^2 R^7} (\eta_{pd\sigma}^2 + \eta_{pd\pi}^2) \\
b_4(R) &= \frac{9\hbar^4 R_d^3}{5\Delta_{pd} m^2 R^7} (\eta_{pd\sigma}^2 - \frac{4}{3}\eta_{pd\pi}^2)
\end{aligned} \tag{5}$$

where  $b_2(R)$  and  $b_4(R)$  are expressed by means of the Harrison parametrization of  $p$ - $d$  hopping. The values of  $\eta_{pd\sigma} = -2.95$  and  $\eta_{pd\pi} = 1.36$  are extracted from his book (first edition).<sup>25</sup> In the case of  $D_{2d}$  symmetry, the distances  $R$ , between magnetic ion and the four ligands are identical.  $\Delta_{pd}$  is the charge transfer energy. It is treated as an adjustable parameter in this theory.

TABLE I: Summary of parameters.

	GaN:Mn		ZnS:Cr	
	our work	experiment <sup>a</sup>	our work	experiment
$\Delta_{5T_2}$ (meV)	187	111	167.1	213.9 <sup>b</sup> 111.6 <sup>c</sup>
$E_{JT}$ (meV)	59.9	37	58.4	71.3 <sup>b</sup> , 37.2 <sup>c</sup>
$\tilde{B}_4^0$ (meV)	-1.88	-1.05	-1.26	
$\tilde{B}_2^0$ (meV)	-8.24	-3.98	-10.15	
$\Delta_q$ (eV)	1.4	1.37	0.57	0.58 <sup>b</sup> , 0.59 <sup>c</sup>
$R$ (Å)	1.932		2.303	
$\delta_x$ (pm)	1.28		1.65	
$\delta_z$ (pm)	3.79		3.46	
$\Delta_{pd}$ (eV)	2.31			
$b_2/b_4$			3.3	

<sup>a</sup>optical measurements for wurtzite GaN:Mn, Wolos *et al*, Ref. 13.

<sup>b</sup>optical measurements, Vallin *et al*, Ref. 26.

<sup>c</sup>optical measurements, Kaminska *et al*, Ref. 14.

Hamiltonian (1) concerns the electronic degrees of freedom only. The tetragonal distortion

results from the coupling to the lattice. As it is shown in Fig. 4 any tetragonal distortion leads to a splitting of the lowest triplet  ${}^5T_2$  and to an energy gain. This energy gain is linear in the lattice displacements, whereas the vibronic energy loss  $E_{vibronic}$  is a quadratic term. One has to minimize the total energy

$$\Delta_{total} = \frac{2}{3} (E({}^5B_2) - E({}^5E_2)) + E_{vibronic} . \quad (6)$$

For the sake of simplicity we approximate  $E_{vibronic}$  by the breathing mode energy, extracted from the LSDA+ $U$  calculation. We find the lattice contribution for GaN:Mn to be  $E_{vibronic}[\text{eV}] = 36.7708R'^2$  and for ZnS:Cr  $E_{vibronic}[\text{eV}] = 30.4887R'^2$  with  $R' = \sqrt{\delta_x^2 + \delta_y^2 + \delta_z^2}$  in Å. One should note, that there is no difference between LSDA and LSDA+ $U$  methods for the lattice energy. Also, we have probed the lattice energy for the more specific tetragonal mode with no essential difference. The energy gain which is induced by the Jahn-Teller effect, corresponds to :

$$E_{JT} = \min(\Delta_{total}) . \quad (7)$$

The results of the ligand field model are presented in Table I. For GaN:Mn, we have exclusively used the ligand hybridization as the microscopic origin for the level splitting. The value of  $\Delta_{pd}$  is adjusted such that  $\Delta_q$  equals the experimental value. The results are very convincing which proves that the exceptional large value of  $\Delta_q = 1.4$  eV in the case of GaN:Mn is dominantly caused by the hybridization energy to the ligands. On the other hand, the neglect of the electrostatic contribution is certainly an approximation which shows its limits for ZnS:Cr. The procedure described above gives no satisfactory results. We interpret this deficiency such that the electrostatic corrections become more important for ZnS:Cr which has a much smaller value of  $\Delta_q$  indicating a smaller hybridization. As discussed in Ref. 27, the higher order crystal field parameters, and especially  $\tilde{B}_4^0$  are certainly more influenced by further reaching neighbors than  $\tilde{B}_4$ . Therefore, we determine the  $b_4$  parameter from the experimentally known value of  $\Delta_q$  and introduce a second free parameter ( $b_2/b_4$ ) which is fitted to the LSDA+ $U$  energy gain. The parameter set for ZnS:Cr which was found in such a manner (Table I) is now in good agreement with previous optical measurements.

TABLE II: Comparison of parameters. When possible, the complete set of parameters was calculated from the literatures values by the relations given in Sect V. HSE : Heyd-Scuseria-Ernzerhof hybrid functional, GGA : Generalized Gradient Aproximation, GFC : Green-function Calculation.

		method	$E_{JT}$ [meV]	$Q_\theta$ [Å]	V [eV/Å]	$\hbar\omega$ [ $cm^{-1}$ ]
GaN:Mn	present work	ligand field theory	59.9	-0.0828	-1.44	579
		ab-initio, LSDA+ $U$	38.13	-0.0562	-1.35	680.5
	literature values	ab-initio, GGA <sup>a</sup>	100	-0.1365	-1.46	454
		ab-initio, HSE <sup>b</sup>	184			
		experiment, optics <sup>c</sup>	37			
ZnS:Cr	present work	ligand field theory	58.4	-0.0834	-1.4	375.8
		ab-initio, LSDA+ $U$	58.4	-0.0496	-2.35	631.5
	literature values	ab-initio, GFC <sup>d</sup>	185.98	-0.16	-2.32	349.4
		experiment, optics <sup>e</sup>	37.2	-0.279	-0.266	90

<sup>a</sup>Luo *et al.* Ref. 18.

<sup>b</sup>Stroppa *et al.* Ref. 12.

<sup>c</sup>Wolos *et al.* Ref. 13, wurzite GaN:Mn.

<sup>d</sup>Oshiyama *et al.* Ref. 30.

<sup>e</sup>Kaminska *et al.* Ref. 14.

## V. COMPARISON TO OTHER WORKS

The lattice displacements obtained from the ligand field theory (Table I) fulfill approximately the relationship  $\delta_x = \delta_y = \frac{1}{2}\delta_z$ . That occurs not by accident since this relationship characterizes a pure tetragonal mode  $Q_\theta$ . In general, up to now, we considered  $\delta_x = \delta_y \neq \delta_z$ , which corresponds to a mixture of tetragonal and breathing mode  $Q_b$  ( $\delta_x = \delta_y = -\delta_z$ ). The normal coordinates of the two modes are defined as  $Q_\theta = -2\sqrt{\frac{2}{3}}(\delta_x + \delta_z)$  and  $Q_b = \frac{2}{\sqrt{3}}(2\delta_x - \delta_z)$ , respectively.<sup>28</sup> But it is only the tetragonal mode which leads to a splitting of the  ${}^5T_2$  level. That is described in the Hamiltonian which was used by Vallin *et al.*<sup>7,14,26</sup> to analyze their data obtained by optical measurements and electron paramagnetic

resonance (EPR)

$$H_D = VQ_\theta\epsilon_\theta + \frac{\kappa}{2}Q_\theta^2. \quad (8)$$

Here, the  $V$  parameter is the Jahn-Teller coupling coefficient, and  $\epsilon_\theta$  is a diagonal 3\*3 matrix which describes the splitting of the  ${}^5T_2$  triplet into the upper  ${}^5E_2$  doublet and the lower  ${}^5B_2$  singlet. Its diagonal elements are 1/2 (corresponding to  ${}^5E_2$ ) and -1 (corresponding to  ${}^5B_2$ ). The parameter  $\kappa$  describes the lattice stiffness and is connected with the phonon frequency by  $\omega = \sqrt{\kappa/m}$  where  $m$  is the mass of one ligand. Minimizing the energy (8) we find the relationship  $V = \kappa Q_\theta$  and the Jahn-Teller energy

$$E_{JT} = \frac{V}{2}Q_\theta. \quad (9)$$

Therefore, if we know the Jahn-Teller energy  $E_{JT}$  and the lattice distortion  $Q_\theta$ , we may calculate the coupling coefficient  $V$  and the phonon frequency  $\omega$  and compare it with other works. The comparison is not an ideal one since our LSDA+ $U$  results do not correspond to a pure tetragonal distortion. They contain an important part of the breathing mode which comes about due to recharging effects around the impurity being not treated in the ligand field theory or in the analysis of the optical data in Refs. 7 and 14. Nevertheless, we compare in Table II our ab-initio and ligand field results with other theoretical or experimental work from the literature. We may remark a rather good agreement for the Jahn-Teller energy  $E_{JT}$  between our work and the optical data of Vallin *et al* for ZnS:Cr.<sup>7</sup> However, our estimate of the phonon frequency is much larger. A detailed analysis of this discrepancy is beyond the scope of the present work. We just remark that higher phonon frequencies would mean a more profound tendency towards the dynamic Jahn-Teller effect. And there are indeed discussions (not for ZnS:Cr, however) whether the experimental data of GaN:Mn should be interpreted as a static<sup>13</sup> or a dynamic<sup>29</sup> Jahn-Teller effect. Such nonadiabatic effects can, however, not at all be treated in density functional based methods.

## VI. DISCUSSION AND CONCLUSION

Many ab-initio studies of Mn-doped GaN or Cr-doped ZnS, mostly based on the LSDA approximation, result in a half-metallic behavior. In those calculations, the Fermi level is located in a small  $3d$  band of majority spin within the middle of the gap of the host semiconductor.<sup>8-11</sup> We have shown, that such a result is an artifact of the LSDA method and can

be repaired by taking into account the strong Coulomb correlation in the  $3d$  shell and the Jahn-Teller effect simultaneously. Allowing for a Jahn-Teller distortion only, but neglecting the Coulomb correlation leads to a tiny gap at the Fermi level.<sup>18</sup> And also the opposite procedure of taking into account the Coulomb correlation by the LSDA+ $U$  method (i.e. the same method which we have used) but remaining in cubic symmetry is insufficient.<sup>31</sup> The origin for this deficiency in the given case of a  $d^4$  impurity is a threefold degenerate level of  $t_{2g}$  symmetry at the Fermi level which is occupied with one electron only. It is sufficient to break the local cubic symmetry in the presence of a strong electron correlation to obtain insulating behavior with a gap of the order of 1 eV. Such an electronic structure is in agreement with the known experimental data for both compounds. Using the LSDA+ $U$  method we found the Jahn-Teller energy gain  $E_{JT}$  in good agreement with known optical data.<sup>13,14</sup>

In addition to the ab-initio calculations, we developed a ligand field theory to reach a deeper understanding of the Jahn-Teller effect. It uses the  $p$ - $d$  hybridization between  $3d$  impurity and ligands as principal origin of the crystal field splitting.<sup>22</sup> This hybridization is parametrized by the Harrison scheme<sup>25</sup> and the lattice energy as obtained from our ab-initio calculation is added. The resulting energy gain is very close to the ab-initio results but the ligand field theory allows in addition the determination of the complete set of crystal field parameters. We find good agreement with the experimental parameter set for GaN:Mn.<sup>13</sup> The comparison is a little bit speculative since the experimental data were obtained for Mn in wurtzite GaN. It turns out, that the Mn impurity leads to an additional tetragonal Jahn-Teller distortion in addition to the intrinsic trigonal deformation of the host lattice. And we find the parameters of this tetragonal distortion close to our results for zinc-blende GaN (which can be synthesized, but for which no measurements exist up to now). We have observed that our ligand field method works better for GaN:Mn than for ZnS:Cr due to the very large cubic crystal field splitting  $\Delta_q = 1.4$  eV in the former case (in contrast to  $\Delta_q = 0.58$  eV for ZnS:Cr).

Our combined ab-initio and analytical study allows also a comparison with the "classical" work on ZnS:Cr. The Jahn-Teller effect of that model compound was already studied in the seventies in great detail by optical and EPR measurements.<sup>7,14,26</sup> We obtain an energy gain  $E_{JT}$  very close to the experimental data but higher phonon frequencies.

Finally, we would like to discuss the importance of our results for spintronics applications.

First of all, the Jahn-Teller mechanism which we describe is not restricted to the two compounds of our study. It may occur in all cases where the impurity level is well separated from the valence band but only partially filled. The Jahn-Teller effect leads to insulating behavior which questions many previous ab-initio studies in the literature. In the case of GaN:Mn all available information points to the stability of  $\text{Mn}^{3+}$  which hinders an intrinsic hole doping by Mn. (Experimentally, one may find  $\text{Mn}^{2+}$  in electron doped samples, which is not well suited for spintronics applications either.) One still has the possibility to reach hole doping by a second impurity besides Mn (co-doping). That would allow the classical mechanism for ferromagnetism in diluted magnetic semiconductors with  $S = 2$  local moments at the Mn sites.

Our work was supported by a PICS project (No. 4767) and we thank Anatoli Stepanov and Andrey Titov for useful discussions.

- 
- <sup>1</sup> T. Dietl, H. Ohno, and F. Matsukura, Phys. Rev. B **63**, 195205 (2001).
  - <sup>2</sup> H. Hori, S. Sonoda, T. Sasaki, Y. Yamamoto, S. Shimizu, K. I. Suga and K. Kindo, Physica B : Condensed Matter **324**, 142 (2002).
  - <sup>3</sup> K. Sato, P. H. Dederichs, K. Araki and H. Katayama-Yoshida, Phys. Stat. Sol. (c) **0**, 2855 (2003).
  - <sup>4</sup> E. Sarigiannidou, F. Wilhelm, E. Monroy, M. Galera, E. Bellet-Amalric, A. Rogalev, J. Goulon, J. Cibert, and H. Mariette Phys. Rev. B **74**, 041306 (R) (2006).
  - <sup>5</sup> T. C. Schulthess, W. M. Temmerman, Z. Szotek, W. H. Butler and G. Malcolm Stocks, Nature Materials **4**, 838 (2005).
  - <sup>6</sup> T. Jungwirth, J. Sinova, A. H. MacDonald, B. L. Gallagher, V. Novák, K. W. Edmonds, A. W. Rushforth, R. P. Champion, C. T. Foxon, L. Eaves, E. Olejnik, J. Mašek, S.-R. Eric Yang, J. Wunderlich, C. Gould, L. W. Molenkamp, T. Dietl, and H. Ohno, Phys. Rev. B **76**, 125206 (2007).
  - <sup>7</sup> J. T. Vallin, G. A. Slack, S. Roberts and A. E. Hughes, Phys. Rev. B **2**, 4313 (1970).
  - <sup>8</sup> B. Sanyal, O. Bengone and S. Mirbt, Phys. Rev. B **68**, 205210 (2003).
  - <sup>9</sup> E. Kulatov, H. Nakayama, H. Mariette, H. Ohta and Y. A. Uspenskii, Phys. Rev. B **66**, 045203 (2002).

- <sup>10</sup> R. D. McNorton, T. M. Schuler, J. M. MacLaren and R. A. Stern, Phys. Rev. B **78**, 075209 (2008).
- <sup>11</sup> C. Tablero, Phys. Rev. B **74**, 195203 (2006).
- <sup>12</sup> A. Stroppa and G. Kresse, Phys. Rev. B **79**, R201201 (2009).
- <sup>13</sup> A. Wolos, A. Wyszomolek, M. Kaminska, A. Twardowski, M. Bockowski, I. Grzegory, S. Porowski and M. Potemski, Phys. Rev. B **70**, 245202 (2004).
- <sup>14</sup> M. Kaminska, J. M. Baranowski, S. M. Uba and J. T. Vallin, J. Phys. C **12**, 2197 (1979).
- <sup>15</sup> K. Koepf and H. Eschrig, Phys. Rev. B **59**, 1743 (1999).
- <sup>16</sup> V. I. Anisimov, J. Zaanen and O. K. Andersen, Phys. Rev. B **44**, 943 (1991).
- <sup>17</sup> M. A. Korotin, V. I. Anisimov, D. I. Khomskii and G. A. Sawatzky, Phys. Rev. Lett. **80**, 4305 (1998).
- <sup>18</sup> X. Luo and R. Martin, Phys. Rev. B **72**, 035212 (2005).
- <sup>19</sup> T. Dietl, Phys. Rev. B **77**, 085208 (2008).
- <sup>20</sup> A. Titov, X. Biquard, D. Halley, S. Kuroda, E. Bellet-Amalric, H. Mariette, J. Cibert, A. E. Merad, G. Merad, M. B. Kanoun, E. Kulatov, and Yu. A. Uspenskii, Phys. Rev. B **72**, 115209 (2005).
- <sup>21</sup> A. Abragam, B. Bleaney, *Electron Paramagnetic Resonance of Transition Ions* (Clarendon Press, Oxford, 1970).
- <sup>22</sup> R. O. Kuzian, A. M. Daré, P. Sati and R. Hayn, Phys. Rev. B **74**, 155201 (2006).
- <sup>23</sup> M.I. Bradbury and D.J. Newman, Chem. Phys. Lett. **1**, 44 (1967). For a review see D.J. Newman and B. Ng, Rep. Prog. Phys. **52**, 699 (1989).
- <sup>24</sup> M.D. Kuzmin, A.I. Popov, and A.K. Zvezdin, Phys. Stat. Sol. (b) **168**, 201 (1991).
- <sup>25</sup> W.A. Harrison, *Electronic Structure and the Properties of Solids* (Freeman, San Francisco, 1980)
- <sup>26</sup> J. T. Vallin and G. D. Watkins, Phys. Rev. B **9**, 2051 (1974).
- <sup>27</sup> A. Savoyant, A. Stepanov, R. Kuzian, C. Deparis, C. Morhain, and K. Graszka, Phys. Rev. B **80**, 115203 (2009).
- <sup>28</sup> M. D. Sturge, Solid State Phys. **20**, 91 (1967).
- <sup>29</sup> S. Marcet, D. Ferrand, D. Halley, S. Kuroda, H. Mariette, E. Gheeraert, F.J. Teran, M.L. Sadowski, R.M. Galera, and J. Cibert, Phys. Rev. B **74**, 125201 (2006).
- <sup>30</sup> A. Oshiyama, N. Hamada and H. Katayama-Yoshida, Phys. Rev. B **37**, 1395 (1988).
- <sup>31</sup> L.M. Sandratskii, P. Bruno, and J. Kudrnovský, Phys. Rev. B **69**, 195203 (2004).